State and Parameter Estimation of a Drift-Flux Model for Under-Balanced Drilling Operations

Amirhossein Nikoofard, Ulf Jakob F. Aarsnes, Tor Arne Johansen, and Glenn-Ole Kaasa

***Abstract*—We consider a drift-flux model (DFM) describing multiphase (gas-liquid) flow during drilling. The DFM uses a specific slip law which allows for transition between single and two phase flows. With this model, we design Unscented and Extended Kalman Filters (UKF and EKF) for estimation of unmeasured state, production, and slip parameters using real time measurements of the bottom-hole pressure, outlet pressure, and outlet flow-rate. The OLGA high-fidelity simulator is used to create two scenarios from Under-Balanced Drilling (UBD) on which the estimators are tested: A pipe connection scenario and a scenario with a changing production index. A performance comparison reveals that both UKF and EKF are capable of identifying the production indices of gas and oil from the reservoir into the well with acceptable accuracy, while the UKF is more accurate than the EKF. Robustness of the UKF and EKF for the pipe connection scenario is studied in case of uncertainties and errors in the reservoir and well parameters of the model. It is found that these methods are very sensitive to errors in the reservoir pore pressure value. However, they are robust in the presence of error in the liquid density value of the model.**

***Index Terms*—Under-balanced drilling, UKF, adaptive observer, simplified drift-flux model, production index.**

I. Introduction

There has been an increasing research focus on automation of drilling for exploration and production of hydrocarbons in the recent years. Modeling for estimation, and model-based control techniques have been studied in a wide range of drilling and production scenarios. In Managed Pressure Drilling (MPD), a back-pressure pump in conjunction with a back pressure choke is used to control the pressure in the well, posing new control and estimation challenges. In a typical scenario, the control goal is to keep the pressure of the well ($p_{\rm well}(t,x)$) greater than pressure of the reservoir ($p_{\rm res}(t,x)$) to prevent influx from entering the well, but lower than the fracture pressure ($p_{\rm frac}(t,x)$) to avoid the loss of drilling fluids to the reservoir [1], [2]

$$p_{\rm res}(t,x) < p_{\rm well}(t,x) < p_{\rm frac}(t,x) \tag{1}$$

at all times t and along the well profile $x \in [0, L]$.

In an alternative approach, known as Under-Balanced Drilling (UBD), the pressure in the well is kept greater than the collapse pressure of the well but lower than the pressure of the reservoir [3]

$$p_{\rm coll}(t,x) < p_{\rm well}(t,x) < p_{\rm res}(t,x) \tag{2}$$

In this case, due to the pressure drawdown (meaning the positive difference of the reservoir pressure and well pressure) inflow fluid, in many cases gas, is produced continuously from the reservoir. The rate of reservoir inflow is typically approximated mathematically by a so-called Production Index (PI) parameter

$$q_{influx} = \text{PI} * \max(p_{\rm res} - p_{\rm bh}, 0). \tag{3}$$

where $p_{\rm bh}$ is the bottom hole pressure. Especially for under-balanced wells producing gas, the magnitude of the production index has a significant impact on the dynamics of the UBD and thus on the control problem as well [4]. Hence, accurate estimation of the production index and reservoir pressure are important for an UBD operation.

Modeling of UBD operations and MPD scenarios handling influx requires a multiphase model. A popular model in the literature is the Drift-Flux Model (DFM) [5], [6], [7]. The drift flux model is a set of first order nonlinear hyperbolic partial differential equations (PDE). In case of two-phase flow, it consists of three governing equations. The Low-Order Lumped (LOL) models are simpler methods that can be used. However, these models are only able to capture the major effects in the well and for the general purpose it produces less accurate results [8], [9], [10].

Due to the complexity of the multi-phase flow dynamics of a UBD well coupled with a reservoir, the modeling, estimation and model based control of UBD operations are still considered emerging and challenging topics within drilling automation. Nygaard et al.[11] compared and evaluated the performance of the extended Kalman filter, the ensemble Kalman filter and the unscented Kalman filter based on a low order model to estimate the states and the production index in UBD operation. In Nygaard et al. [12], a finite horizon nonlinear model predictive control in combination with an unscented Kalman filter was designed for controlling the bottom-hole pressure based on a low order model developed in [8] for a pipe connection scenario. The unscented Kalman filter was used to estimate the states, and the friction and choke coefficients. Nikoofard et al.[9] designed a Lyapunov-based adaptive observer, a recursive least squares estimation and a joint unscented Kalman filter based on a low-order lumped model to estimate states and parameters during UBD operations. This model was the extended version of an adaptive observer used in [9] for directly using real-time measurements of the choke and the bottom-hole pressures to estimate states

Amirhossein Nikoofard and Tor Arne Johansen are with the Center for Autonomous Marine Operations and Systems, Department of Engineering Cybernetics, Norwegian University of Science and Technology, Trondheim, Norway. E-mail: Amirhossein.nikoofard@ntnu.no, Tor.arne.johansen@itk.ntnu.no

Ulf Jakob F. Aarsnes is with the Department of Engineering Cybernetics, Norwegian University of Science and Technology, Trondheim, Norway, and the DrillWell, International Research Institute of Stavanger, Oslo, Norway. E-mail: ujfa@iris.no

Glenn-Ole Kaasa is both with Kelda Drilling Controls, Porsgrunn, Norway, and the Department of Engineering Cybernetics, Norwegian University of Science and Technology, Trondheim, Norway.E-mail: gok@kelda.no

and parameters [13]. The performance of the adaptive observers was compared and evaluated for a typical drilling case to estimate only production index of gas using a simulated scenario with a drift-flux model. A Nonlinear Moving Horizon Observer based on a low-order lumped model was designed for estimating the total mass of gas and liquid in the annulus and geological properties of the reservoir during UBD operation in [14].

Lorentzen et al. designed an ensemble Kalman filter based on the drift-flux model to tune the uncertain parameters of a two-phase flow model in the UBD operation [6]. Vefring et al.[15], [16] compared and evaluated the performance of the ensemble Kalman filter and an off-line nonlinear least squares technique utilizing the Levenberg-Marquardt optimization algorithm to estimate reservoir pore pressure and reservoir permeability during UBD while performing an excitation of the bottom-hole pressure. The result shows that excitation of the bottom-hole pressure might improve the estimation of the reservoir pore pressure and reservoir permeability [15], [16]. Aarsnes et al.[17] used a drift-flux model and an Extended Kalman Filter to estimate the states and production index online, and suggested a scheme combining this with off-line calibration using the algorithm in [15]. The provided analysis also suggests how such a scheme fits into the UBD operating envelope as proposed by [18], and explored in [19]. Di Meglio et al. designed an adaptive observer based on a backstepping approach for a linear first-order hyperbolic system of Partial Differential Equations (PDEs) by using only boundary measurements with application to UBD [20]. It is shown that this method has exponential convergence for the distributed state and the parameter estimation. This adaptive observer is applied to estimate distributed states and unknown boundary parameters of the well during UBD operations. Gao Li et al. presented an algorithm for characterizing reservoir pore pressure and reservoir permeability during UBD of horizontal wells [21]. Since the total flow rate from the reservoir has a negative linear correlation with the bottom hole pressure, reservoir pore pressure can be identified by the crossing of the horizontal axis and the best-fit regression line between the total flow rate from the reservoir and the bottom hole pressure while performing an excitation of the bottom-hole pressure by changing the choke valve opening or pump rates. The unscented Kalman filter (UKF) has been shown to typically have a better performance than other Kalman filter techniques for nonlinear systems ([22], [23]). Nikoofard et al. used an UKF with the drift-flux model for the first time [24]. They designed an UKF for estimation of unmeasured states, production and slip parameters of simplified drift-flux model using real time measurements of the bottom-hole pressure and liquid and gas rate at the outlet [24]. This paper is an extended version of work published in [24] which presents the design of a UKF based on a simplified drift-flux model to estimate the states, geological properties of the reservoir and slip parameters during UBD operation. In this work, both production indices of gas and liquid and unmeasured states are estimated by using only measurements of the choke and the bottom-hole pressures during UBD operation for a pipe connection procedure. In this paper, it is assumed that the electromagnetic measurement while drilling (MWD) is used for the telemetry system. The performance of UKF is evaluated against EKF by using measurements from the OLGA simulator and the consequences of not estimating slip parameters are discussed. These adaptive observers were tested by two challenging scenarios:

1) Changing the production index of gas.
2) Pipe connection.

The performance of the estimation algorithms to detect and track the change in production parameters is investigated. The main purpose of the paper is to estimate production indices of gas and liquid during UBD operations for different scenarios and different conditions such as working with a manual or automatic controller. In addition, this study assesses the effect of the discretization, the choice of estimated parameters, effect of measurements on the simulated estimation algorithms. Robustness of the estimators for the pipe connection scenario is studied in case of uncertainties and errors in the reservoir and well parameters of the model. This paper is organized as follows: Section II presents the simplified drift-flux model based on mass and momentum balances for UBD operation. Section III explains UKF and EKF for simultaneously estimating the states and parameters of a simplified drift-flux model from OLGA simulator measurements. In the section IV, the simulation results are provided for state and parameter estimation. The conclusions are presented at the end of the paper.

II. The drift flux model

The model employed is the same as the one used in [19]. It expresses the mass conservation law for the gas and the liquid separately, and a combined momentum equation. The mud, oil and water are lumped into one single liquid phase. In developing the model, the following mass variables are used

$$m = \alpha_L \rho_L, \qquad n = \alpha_G \rho_G$$

where for $k = L, G$ denoting liquid or gas, ρ_k is the phase density, and α_k is the volume fraction satisfying

$$\alpha_L + \alpha_G = 1. \tag{4}$$

Further v_k denotes the velocities, and P the pressure. All of these variables are functions of time and space. We denote $t \geq 0$ the time variable, and $x \in [0, L]$ the space variable, corresponding to a curvilinear abscissa with x = 0 corresponding to the bottom hole and x = L to the outlet choke position (see Fig. 1). The isothermal equations are as follows,

$$\frac{\partial m}{\partial t} + \frac{\partial m v_L}{\partial x} = 0, \tag{5}$$

$$\frac{\partial n}{\partial t} + \frac{\partial n v_G}{\partial x} = 0, \tag{6}$$

$$\frac{\partial (m v_L + n v_G)}{\partial t} + \frac{\partial (P + m v_L^2 + n v_G^2)}{\partial x} = -(m+n) g \cos \Delta\theta - \frac{2 f (m+n) v_m |v_m|}{D}. \tag{7}$$

In the momentum equation (7), the term $(m + n)g \cos \Delta\theta$ represents the gravitational source term, g is the gravitational

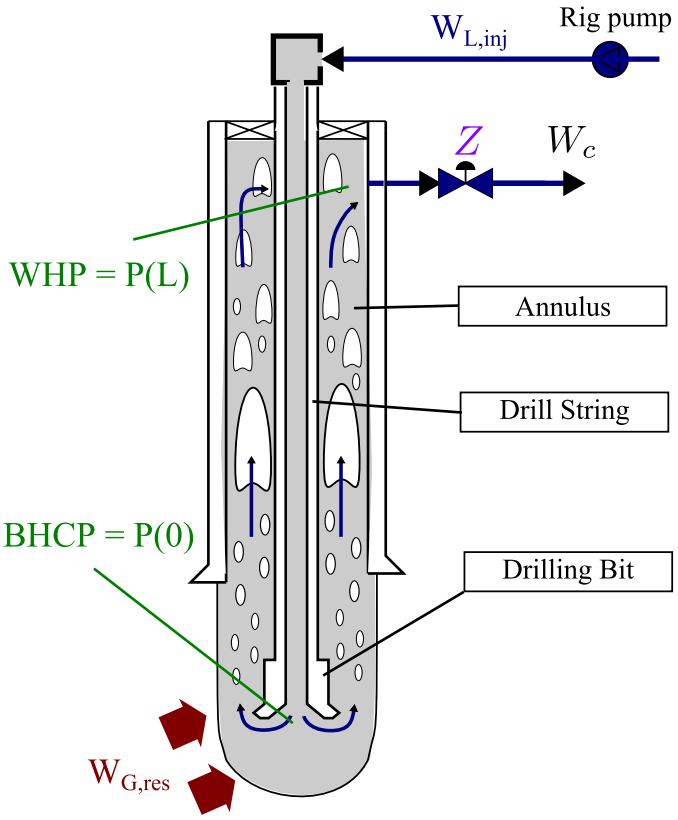

Fig. 1. Drilling process schematic for UBD.

constant and $\Delta\theta$ is the mean angle between gravity and the positive flow direction of the well, while $-\frac{-2f(m+n)v_m|v_m|}{D}$ accounts for frictional losses. The mixture velocity is given as

$$v_m = \alpha_G v_G + \alpha_L v_L. \tag{8}$$

Along with these distributed equations, algebraic relations are needed to describe the system.

A. Closure Relations

Both the liquid and gas phase are assumed compressible. This is required for the model to handle the transition from two-phase to single-phase flow. The densities are thus given as functions of the pressure as follows

$$\rho_G = \frac{P}{c_G^2}, \qquad \rho_L = \rho_{L,0} + \frac{P}{c_L^2}, \tag{9}$$

where c_k is the velocity of sound and $\rho_{L,0}$ is the reference density of the liquid phase given at vacuum. Note that the velocity of sound in the gas phase c_G depends on the temperature as suggested by the ideal gas law. The temperature profile is assumed to be known.
Combining (9) with (4) yields the following equalities that can be exploited to find the volume fractions as a function of mass variables:

$$\alpha_G = \frac{1}{2} - \frac{\frac{c_G^2}{c_L^2}n + m + \sqrt{\Delta}}{2\rho_{L,0}}, \tag{10}$$

$$\Delta = \left(\rho_{L,0} - \frac{c_G^2}{c_L^2}n - m\right)^2 + 4\frac{c_G^2}{c_L^2}n\rho_{L,0} \tag{11}$$

Then the pressure can be found using a modified expression to ensure pressure is defined when the gas vanishes

$$P = \begin{cases} \left(\frac{m}{1-\alpha_G} - \rho_{L,0}\right)c_L^2, & \text{if } \alpha_G \le \alpha_G^* \\ \frac{n}{\alpha_G}c_G^2, & \text{otherwise,} \end{cases} \tag{12}$$

Note that the above two expressions are equivalent except for the singularities occurring at 0 and 1, respectively. Hence α_G^* can be set to any value $\alpha_G^* \in (0,1)$ [19]. Because the momentum equation (7) was written for the gas-liquid mixture, a so-called *slip law* is needed to empirically relate the velocities of gas and liquid. To handle the transition between single and two-phase flow, a relation with state-dependent parameters is needed ([25], [26]).

$$v_G = (K - (K-1)\alpha_G)v_m + \alpha_L S \tag{13}$$

where $K \ge 1$ and $S \ge 0$ are constant parameters.

B. Boundary Conditions

Boundary conditions are given by the mass-rates of gas and liquid injected from the drilling rig and flowing in from the reservoir. Denoting the cross sectional flow area by A, the boundary fluxes are given as:

$$mv_L|_{x=0} = \frac{1}{A}\Big(W_{L,res}(t) + W_{L,inj}(t)\Big), \tag{14}$$

$$nv_G|_{x=0} = \frac{1}{A}\Big(W_{G,res}(t) + W_{G,inj}(t)\Big). \tag{15}$$

The injection mass-rates of gas and liquid, $W_{G,inj}, W_{L,inj}$, are specified by the driller and can, within some constraints, be considered as manipulated variables. The inflow from the reservoir is dependent on the pressure on the left boundary, for which, within the operational range of a typical UBD operation, an affine approximation should suffice, i.e.

$$W_{L,res} = k_L \max(P_{res} - P(0), 0) \tag{16}$$

$$W_{G,res} = k_G \max(P_{res} - P(0), 0) \tag{17}$$

Here P_{res} is the reservoir pore pressure and k_G, k_L are the production index of the gas and liquid respectively.

The topside boundary condition is given by a choke equation relating topside pressure to mass flow rates

$$\frac{mv_L}{\sqrt{\rho_L}} + \frac{nv_G}{Y\sqrt{\rho_G}}\Big|_{x=L} = \frac{C_v(Z)}{A}\sqrt{\max\left(P(L,t) - P_s, 0\right)}, \tag{18}$$

where C_v is the choke opening given by the manipulated variable Z. $Y \in [0,1]$ is a gas expansion factor for the gas flow and P_s is the separator pressure, i.e. the pressure downstream the choke.

C. Numerical Implementation

The drift flux model described above was implemented using a fully implicit Backwards Time-Central Space (BTCS) finite differences numerical scheme with an explicitly derived Jacobian as described in [19].

The state vector consists of the conserved mass variables m and n and the combined momentum $I = mv_L + nv_G$, $X =$

$\begin{bmatrix} m & n & I \end{bmatrix}^T$. For each of the states it is used the following definition for finite differences,

$$m_i^k = m(k\Delta t, i\Delta x), \quad \text{etc.}$$

where $i = 0, 1, \ldots, N$ and $k = 0, 1, \ldots$. It is arranged the terms into a vector

$$X_k = \left[m_1^k, m_2^k, \ldots, m_N^k, n_1^k, \ldots, n_N^k, I_1^k, \ldots, I_N^k\right].$$

Consequently, propagating the states in time from X_k to X_{k+1} equates to solving a set of nonlinear equations that are implicit in X_{k+1}, which it is denoted as

$$F(X_{k+1}, X_k) = 0, \qquad F : \mathbb{R}^{3N} \times \mathbb{R}^{3N} \to \mathbb{R}^{3N}. \tag{19}$$

These are solved using Newton steps which require the inverse of the Jacobian of F w.r.t. X_{k+1} denoted $F_{X_{k+1}}$. We note that the existence of this inverse is guaranteed by the $1/\Delta t$ terms making up the diagonal of $F_{X_{k+1}}$.

III. Unscented and Extended Kalman Filter

A. UKF

The implemented drift-flux model based on equations (5)-(18), although solved implicitly, can conceptually be represented as

$$X_k = f(X_{k-1}, \theta) + q_k \tag{20}$$

$$y_k = h(X_k) + r_k \tag{21}$$

where $q_k \sim N(0, Q_{k-1})$ is the zero mean white Gaussian process noise and model error, and $r_k \sim N(0, R_k)$ is the zero mean white Gaussian measurement noise. y_k is a set of measurements from the model and θ is the set of unknown parameters of the model that must be estimated. y_k and θ for each scenario are defined and discussed in section IV.
The Kalman filter based on a linearized model was developed to estimate both state and parameter of the system usually known as an augmented Kalman filter. The augmented state vector is defined by $x^a = [X, \theta]$. The state-space equations for the augmented state vector at time instant k are written as:

$$\begin{bmatrix} X_k \\ \theta_k \end{bmatrix} = \begin{bmatrix} f(X_{k-1}, \theta_{k-1}) + q_k \\ \theta_{k-1} \end{bmatrix} = f^a(X_{k-1}, \theta_{k-1}) + q_k^a \tag{22}$$

The UKF technique has been developed to work with non-linear systems without using an explicit linearization of the model ([27], [28], [29]). The UKF estimates the mean and covariance matrix of the estimation error with a minimal set of sample points (called sigma points) around the mean by using a deterministic sampling approach known as the unscented transform. The nonlinear model is applied to sigma points to predict uncertainty instead of using a linearization of the model. More details can be found in ([28], [29], [22]).

Dual and joint UKF techniques are two common approaches for estimation of parameters and state variables simultaneously. The dual UKF method uses another UKF for parameter estimation so that two filters run sequentially in every time step; the state estimator updates with new measurements, and then the current estimate of the state is used in the parameter estimator. The joint UKF augments the original state variables with parameters and a single UKF is used to estimate augmented state vector.

In this paper, the joint UKF is used.

B. EKF

For the implementation of an Extended Kalman Filter,to be used for comparison we need the Jacobian of the explicit formulation of the system equation. A first order Taylor series expansion around the trajectory $\bar{X}$, noting that $F(\bar{X}_{k+1}, \bar{X}_k) = 0$, yields

$$F_{X_{k+1}}(\bar{X}_{k+1}, \bar{X}_k)\tilde{X}_{k+1} + F_{X_k}(\bar{X}_{k+1}, \bar{X}_k)\tilde{X}_k = 0. \tag{23}$$

where $F_{X_k}(\bar{X}_{k+1}, \bar{X}_k)$ is F with respect to a X_k. Hence, for the system Jacobian, this gives

$$J = -F_{X_{k+1}}^{-1}(\bar{X}_{k+1}, \bar{X}_k)F_{X_k}(\bar{X}_{k+1}, \bar{X}_k)$$

where the partial derivatives are evaluated at the trajectory. We recognize $F_{X_{k+1}}$ to be the Jacobian, previously discussed, the inverse of which is known to exist.

IV. Simulation results

A. Simulation with perfect model data

First, the presented DFM, (5)-(15) was used to create the measurements and true states in this simulation study. In this case the estimated states and parameters, in several configurations of unknown parameters to be estimated, converged to the true states (results not shown). Convergence transients were typically 0.5 hours for the UKF and 1.5 hours for the EKF. Of significantly more interest, however, is how the estimators performs in a more realistic setting where we would have model errors to deal with. Such a scenario is considered next.

B. Case 1: Tracking production index

In starting a UBD operation, estimates of reservoir pressure are provided to the driller by reservoir engineers ahead of time and these are updated during the operation by performing flow tests. The reservoir pressure is then assumed reasonably homogeneous in time as one is drilling through the same reservoir, while the production index increases as progressively larger parts of the production matrix is opened up and the drilling bit potentially encounters faults [30], [31].

As such, a scenario is considered where the reservoir pressure is assumed known and the performance of the estimation algorithm is evaluated by its ability to track a rapid change in the production index.

1) Parameter values and OLGA setup: The parameter values for the simulated well and reservoir are summarized in Table I. These parameters are used from the OLGA simulator. The OLGA dynamic multiphase flow simulator is a high fidelity simulation tool which has become the de-facto industry standard in oil and gas production, see [32]. The measurements have been synthetically generated by using OLGA. The OLGA simulator uses the same model for the mass flow from the reservoir into the well as in equations (16)-(17).

In the following, a measurement sampling interval of 10

TABLE I
PARAMETER VALUES FOR WELL AND RESERVOIR

Name	DFM	Unit
Reservoir pressure (p_{res})	279	bar
Collapse pressure (p_{coll})	155	bar
Well total length (L_{tot})	2530	m
Drill string outer diameter (D_d)	0.1206	m
Well inner diameter (D_a)	0.1524	m
Liquid flow rate ($w_{l,d}$)	13.33	kg/s
Gas flow rate ($w_{g,d}$)	0	kg/s
Liquid density (ρ_L)	1000	$\mathrm{kg/m^3}$
Gas average temperature (T)	285.15	K
Average angle ($\Delta\theta$)	0	rad
Choke constant (K_c)	0.0053	$\mathrm{m^2}$

TABLE II
CHOKE OPENING USED IN THIS SCENARIO

Time	Choke Opening
0-1 h	10 %
1-2 h	8 %
2-6 h	7 %
6-8 h	6 %
8-10 h	5.5 %

seconds was used, and the model was run with time steps of 10 seconds using different number of spatial discretization cells ($N = 6, 12, 20$).

Two scenarios are simulated. The first scenario of this paper is the same simulation scenario as [17], considering UBD operation of a vertical well drilled into a dry gas reservoir (i.e. $W_{L,res} = K_L = 0$). The scenario in this simulation is as follows. First drilling in a steady-state condition is initiated with the choke opening of 10 % , then the choke is closed to 8 % at 1 hour. After 2 hours, the choke is closed to 7 %. After 3.5 hours, there is a linear and sharp increase in the production index of gas from 0.072 kg/s/bar to 0.12 kg/s/bar. Then the choke is closed to 6 % at 6 hours, and after 8 hours, the choke is closed to 5.5 %. The choke opening of this simulation scenario is summarized in Table II.

In the first scenario, it is assumed that only bottom-hole pressure ($P(0)$) and liquid and gas rate at the outlet are measured. The joint UKF and EKF estimate the states, production index of gas, and slip parameters (S, K) simultaneously. The initial value for the estimated production index of gas is ($\hat{K_G} = 0.08$ kg/s/bar). UKF parameters are determined empirically ($\kappa = 0$, $\beta = 2$, $\alpha = 0.00001$). Note that α can be set to any small positive value (e.g., $\alpha \leq 1$) [29]. The measurement noise covariance matrix is $R = diag[0.01, 0.0004, 0.04]$. The covariance matrix used in this simulation for both EKF and UKF is

$$Q = diag[Q_s, Q_p]$$
$$Q_p = diag[10^{-3}, 2 * 10^{-6}, 2 * 10^{-5}] \ , \ p = [K_G, K, S]$$

where Q_s and Q_p are the state covariance and parameter covariance matrices, respectively. We used the same the state covariance matrix for two scenarios. Choosing process noise in the UKF or EKF (Q) specifies trade-offs in the UKF or EKF design. Choosing larger process noise in the UKF or EKF (Q) leads to faster track of data and convergence but more uncertainty in the estimation. Choosing smaller process noise in the UKF or EKF (Q) leads to slower track of data and convergence but less uncertainty in the estimation. In this paper, it is shown that this choice of covariance matrix (Q) gives reasonable performance of the estimator algorithms, but we emphasize that the covariance matrix (Q) is not tuned to optimize the performances.

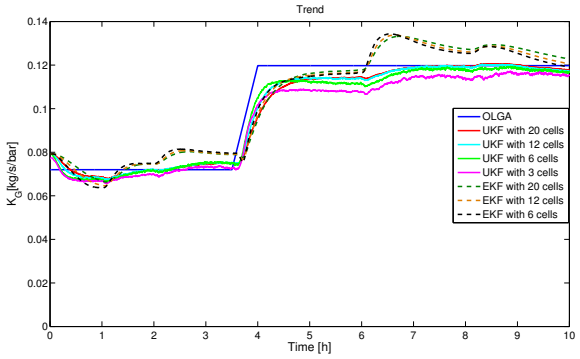

Fig. 2. Estimating production index of gas with different number of spatial discretization cells.

The reason the slip parameters K, S are empirical closure relations without direct physical interpretations [33]. This means that there is no correct value for the parameter estimation to converge to, but they are included in the hope that they can compensate for the model errors resulting from the simplifying assumptions behind the DFM, thereby potentially improving the estimation of other parameters (namely production index).

2) Simulation results and discussion: The estimations of the production index of gas from the reservoir into the well for different spatial discretizations for both UKF and EKF are shown in Figure 2. The estimation algorithms are quite fast to detect and track changing at production index of gas. However, there is a small deviation between the estimated and actual value of the production index of gas. The number of steps in the spatial discretization does not have a significant effect on the accuracy of estimation, although the results show that decreasing number of steps can improve the convergence rate.

Figures 3 and 4 show the estimated slip parameters K and S for different spatial discretization cells for both UKF and EKF, respectively. The estimation of slip parameters for the UKF seems to converge slowly, or not at all. However, estimation of production index of gas has some errors during most of the scenario. On the other hand, estimation of production index of gas in UKF has less error. In this case estimation of slip parameters varies during steady state. Since slip parameters are artificial parameters and has no reference value their convergence may not be important. As a production index is a physical parameter, the convergence for estimation of production index is vital for success of UBD operations.

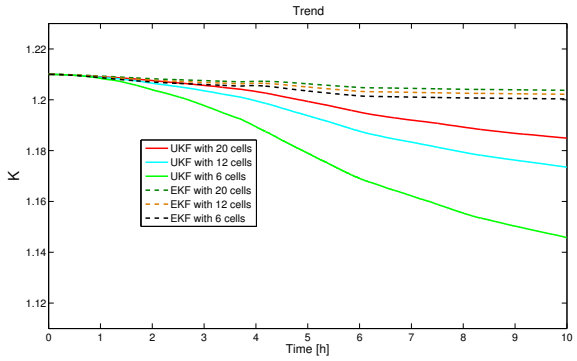

Fig. 3. Estimating slip parameter (K) for different number of spatial discretization cells.

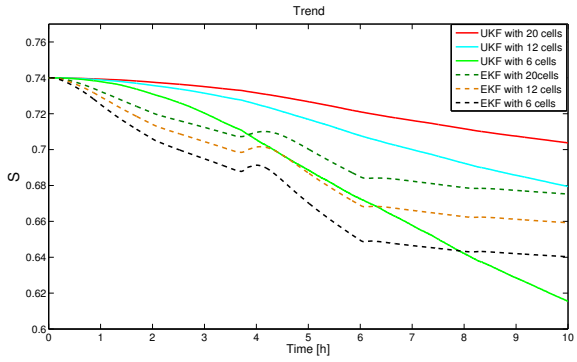

Fig. 4. Estimating slip parameter (S) for different number of spatial discretization cells.

Figure 5 shows the estimation of the production index of gas with different fixed slip parameters by using UKF with 6 spatial discretization cells. The results show that estimation of the slip parameters can improve accuracy of the estimation of the production index of gas. The measured bottom-hole pressure and choke pressures are illustrated in Figure 6.

The runtime of the simulations for different spatial discretization cells for both UKF and EKF are summarized in Table III by using 3.00 GHz Processor with 4 GB RAM

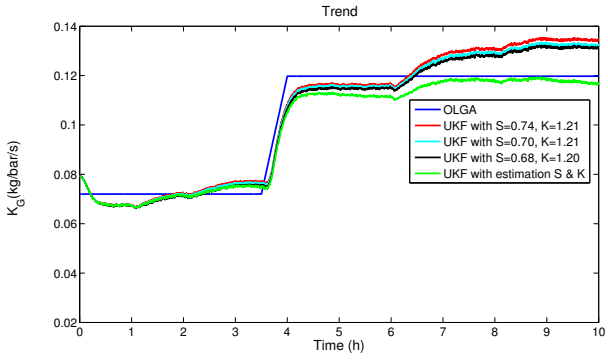

Fig. 5. Estimating production index of gas with fixed slip parameters.

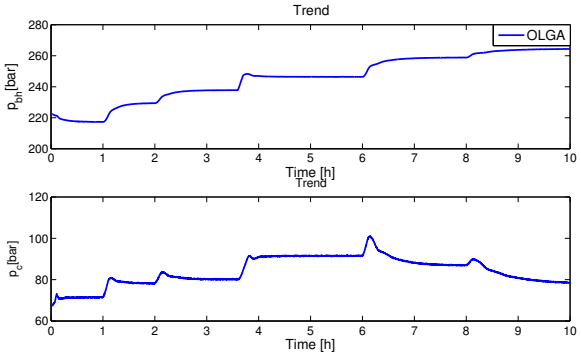

Fig. 6. Bottom-hole pressure and choke pressure

TABLE III
SIMULATION RUNTIME FOR DIFFERENT NUMBER OF SPATIAL DISCRETIZATION CELLS.

Number of Cells	UKF (seconds)	EKF(seconds)
6	630.38	63.88
12	1110.82	67.27
20	2326.35	78.16

running MATLAB, the runtime of the simulations for EKF are less than the runtime of the simulations for UKF, but we emphasize that the implementation is not optimized for computational efficiency.

Performance of these adaptive observers is evaluated through the root mean square error (RMSE) metric for the parameter K_G. The RMSE metric for UKF and EKF for different number of spatial discretization cells is summarized in Table IV.

TABLE IV
RMSE METRIC FOR ESTIMATE OF K_G

Number of Cells	UKF	EKF
3	7.3×10^{-3}	9.4×10^{-3}
6	4.8×10^{-3}	8.2×10^{-3}
12	4.8×10^{-3}	8×10^{-3}
20	5.16×10^{-3}	8.3×10^{-3}

According to the RMSE metric table, UKF with fewer cells in the spatial discretization has a slightly better performance than UKF with larger number of spatial discretization cells and EKF with different number of spatial discretization cells for production index estimation, although the number of cells in the spatial discretization does not have a significant effect on the accuracy of estimation. If the number of cells is slightly more than a minimum number (5 or 6 spatial discretization cells for this case) we can get satisfactory results from the estimator.

The total effective model error is due to a combination of error in the mathematical model and error introduced by the discretization. With regards to a given variable, these errors might be compounded or they might partially cancel each other. Hence it is possible that reducing the number of cells in the discretization may yield an improved performance for a given case. Of course, this does not mean that reducing the

number of cells will always improve performance, however, this point can be used to argue for using low order approximations as the largest cause of error is often due to the errors in the mathematical model and not due to the discretization.

C. Case 2: Pipe connection

The second case study that is reported in this paper considers UBD operation of a vertical well drilled into an oil and gas reservoir. First the drilling in a steady-state condition is initiated with the choke opening of 10 %, then at t = 1 hour and 35 min the main pump is shut off to perform a connection procedure, and the choke is closed to 6 %. The rotation of the drill string and the circulation of fluids are stopped for 15 mins. Next after making the first pipe connection at t = 1 hour and 50 min the main pump and rotation of the drill string are restarted. After 1 hour and 45 min (i.e. 3 hour and 35 min), the choke is closed to 5 %, and the second pipe connection procedure is started, and is completed after 15 mins. Then the choke is opened to 10 % at t= 3 hours and 50 min. The measured bottom-hole pressure (p_{bh}), choke pressure (p_c), choke opening (Z), and mass flow rate of liquid from the drill string ($w_{l,d}$) are illustrated in Figure 7.

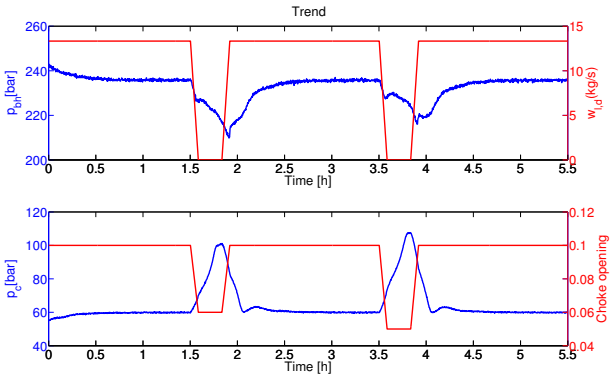

Fig. 7. Measured bottom-hole pressure, choke pressure, choke opening, and mass flow rate of liquid from the drill string for pipe connection scenario.

Since these two scenarios model two drilling cases with different specifications, different measurements and different parameters for each scenario was used. Due to the fact that the liquid and gas flow rate at the outlet are sometimes measured by flow meter after separator, these measurements have usually some delay. Also, these measurements are sometimes not available. Therefore, the purpose of the second scenario is to show how the estimator works without these measurements. This way we can answer a wide range of problems in UBD operation with choosing different measurements by using these two scenarios.

1) Case 2a: Pipe connection with manual controller: In the second scenario, it is assumed that only bottom-hole pressure ($P(0)$) and choke pressure ($P(L)$) are measured. The UKF estimates the states and production indices of gas and liquid (K_G, K_L). Since slip parameters can be estimated only by measurement of the liquid and gas flow rate, slip parameters in this simulation are fixed ($K = 1.15, S = 0.56$). The parameter values for the UKF for pipe connection scenario are the same

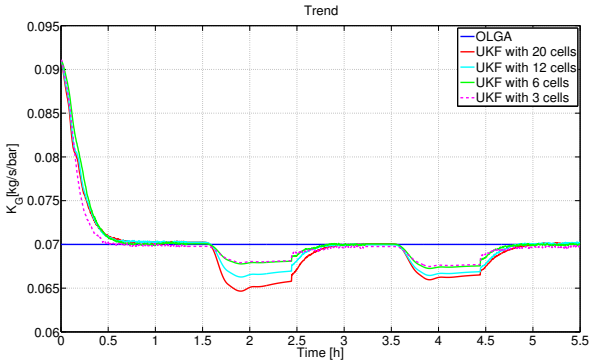

Fig. 8. Estimating gas production index of gas with different number of spatial discretization cells during a pipe connection.

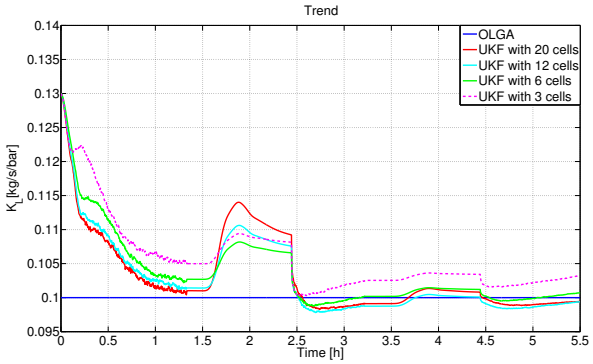

Fig. 9. Estimating liquid production index with different number of spatial discretization cells during a pipe connection.

as previous scenario. The initial values for the estimated and real parameters are as follows:

$$K_G = 0.07, \quad K_L = 0.1, \quad \hat{K_G} = 0.091, \quad \hat{K_L} = 0.13$$

The bottom-hole and the choke pressure measurements are corrupted by zero mean additive white noise with the following covariance matrix

$$R = \begin{bmatrix} 0.9 * 0.4^2 & 0 \\ 0 & 0.9 * 0.2^2 \end{bmatrix} (bar^2)$$

The covariance matrix for parameter variations uses in this simulation for both EKF and UKF is

$$Q_p = diag[4 * 10^{-4}, 2 * 10^{-3}], \quad p = [K_G, K_L].$$

Figures 8 and 9 show the estimated production indices of gas and liquid from the reservoir into the well for different spatial discretization cells for UKF, respectively.

The RMSE metric of the parameters K_G and K_L for UKF and EKF for different spatial discretization cells after initial transient ($t \geq 0.5hour$) are summarized in Table V. The results show that UKF and EKF with fewer cells in the spatial discretization for the estimation of gas and liquid production indices have a better accuracy than UKF and EKF with larger spatial discretization cells with different spatial discretization cells for the estimation of gas and liquid production indices during the pipe connection. Since the model is significantly less accurate during the pipe connection, we need to prevent

TABLE V
RMSE METRIC FOR ESTIMATE OF K_G AND K_L FOR PIPE CONNECTION SCENARIO WITHOUT CONTROLLER

Number of Cells	K_G (after $t \geq 0.5h$)		K_L (after $t \geq 0.5h$)	
	UKF	EKF	UKF	EKF
3	1.3×10^{-3}	1.4×10^{-3}	5.0×10^{-3}	5.2×10^{-3}
6	1.4×10^{-3}	1.5×10^{-3}	3.6×10^{-3}	3.6×10^{-3}
12	1.8×10^{-3}	2.2×10^{-3}	3.8×10^{-3}	3.8×10^{-3}
20	2.4×10^{-3}	3.1×10^{-3}	4.8×10^{-3}	4.9×10^{-3}

that the production index estimates drift away in order to compensate for other model errors. Hence, the Q_p of UKF and EKF is 1000 times smaller than the nominal value during the pipe connection. For the same reason, the measurement covariance of UKF and EKF is tuned 1000 times larger than the nominal value during the pipe connection.

The RMSE metric shown in Table V, shows the same trend as previous case, where the UKF with fewer cells in the spatial discretization for the estimation of gas production index (K_G) has a slightly better performance than the UKF with larger spatial discretization cells and the EKF with different spatial discretization cells, for the estimation of K_G. This can be explained by considering the fact that there are two potential sources of error: model error, and numerical error due to discretization. In most cases, reducing the numerical error by increasing the number of cells will reduce the total error. However, there is an optimum number of cells that has better performance compared to smaller or larger number of cells. It is possible that two sources of error can, to some degree, cancel each other out which is the case here. Based on the above mentioned reason, it can be concluded that increasing the number of cells beyond a certain point will result in small increase in performance as the model error will start to dominate over the numerical.

2) Case 2b: Pipe connection with PI controller: For automated control of bottom hole pressure, a PI controller was applied to the drilling system for pipe connection scenario. This controller creates a dynamic mapping from the bottom hole pressure to the choke opening Z in (18). The PI controller is popular as an industrial controller and easy to tune. Proportional and integral gains are chosen as 0.01 and 0.0002, respectively. For more details on how the PI controller can be designed and tuned for this scenario the interested reader is referred to [33], [34], [35]. The parameter values for the UKF are the same as previous scenario.The measured bottom-hole pressure (p_{bh}) and choke pressure (p_c) for pipe connection scenario with PI controller is illustrated in Figure 10. Figure 11 shows the choke opening for pipe connection scenario with PI controller.

Figures 12 and 13 show the estimated production indices of gas and liquid from the reservoir into the well with PI controller for pipe connection scenario by using UKF with 6 spatial discretization cells, respectively.

The RMSE metric of the parameters K_G and K_L for UKF for different spatial discretization cells after initial transient ($t \geq 0.5hour$) are summarized in Table VI. The results show that PI controller can improve accuracy of the estimation of

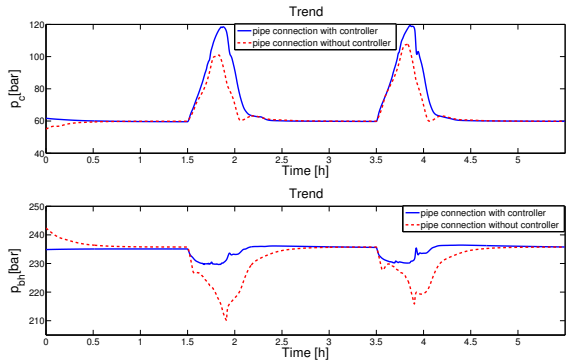

Fig. 10. Measured bottom-hole pressure and choke pressure for pipe connection scenario with PI controller.

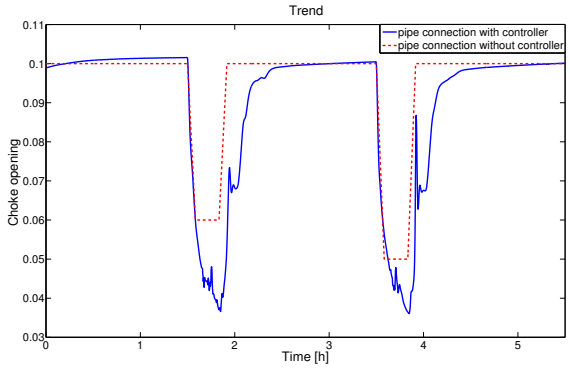

Fig. 11. Choke opening for pipe connection scenario with PI controller.

the production indices of gas and liquid due to reducing the disturbance of pipe connection.

3) Case 2c: Robustness analysis of UKF and EKF in case of uncertainties and errors in the reservoir and well parameters of the model: Robustness of the adaptive observers is investigated in case of errors in the reservoir and well parameters of the model. This test is performed in case of errors in the reservoir pore pressure and liquid density for pipe connection scenario. The RMSE metric for UKF and EKF in the two cases of 1% error on the reservoir pore pressure ($p_{res,model} = 282$ bar) and 10% error on the liquid density ($\rho_{L,model} = 1100$ kg/m^3) for different spatial discretization cells after initial transient ($t \geq 0.5hour$) are summarized in Table VII and VIII, respectively.

Since the reservoir pore pressure has a direct effect on the mass flow rates from the reservoir into the well, small inaccuracies in the reservoir pore pressure have a significant

TABLE VI
RMSE METRIC FOR ESTIMATE OF K_G AND K_L FOR PIPE CONNECTION SCENARIO WITH PI CONTROLLER.

Number of Cells	K_G (after $t \geq 0.5h$)	K_L (after $t \geq 0.5h$)
6	0.6×10^{-3}	1.3×10^{-3}
12	0.85×10^{-3}	1.1×10^{-3}
20	1.1×10^{-3}	1.4×10^{-3}

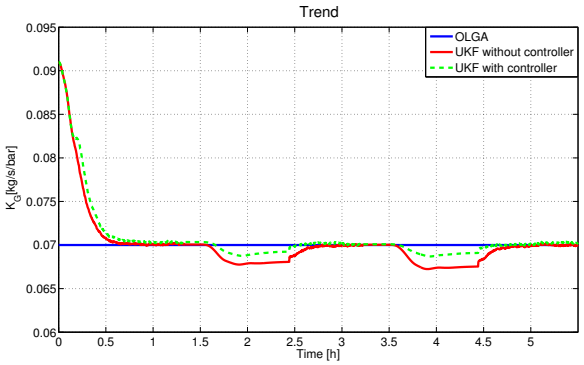

Fig. 12. Estimating production index of gas for pipe connection with PI controller

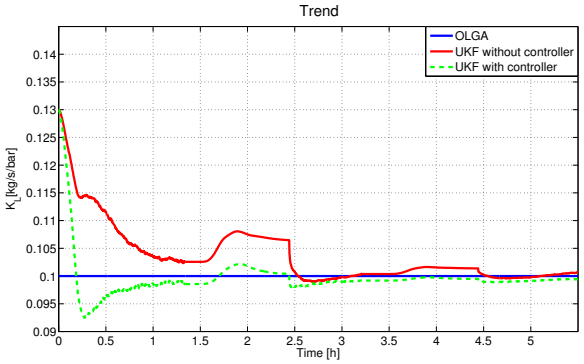

Fig. 13. Estimating liquid production index for pipe connection with PI controller.

TABLE VII
RMSE METRIC IN CASE OF ERROR IN THE RESERVOIR PRESSURE VALUE FOR PIPE CONNECTION SCENARIO WITHOUT CONTROLLER

Number of Cells	K_G (after $t \geq 0.5h$)		K_L (after $t \geq 0.5h$)	
	UKF	EKF	UKF	EKF
6	5.4×10^{-3}	5.6×10^{-3}	5.2×10^{-3}	5.3×10^{-3}
12	5.8×10^{-3}	6.0×10^{-3}	6.0×10^{-3}	6.0×10^{-3}
20	6.2×10^{-3}	6.7×10^{-3}	6.1×10^{-3}	6.3×10^{-3}

TABLE VIII
RMSE METRIC IN CASE OF ERROR IN THE LIQUID DENSITY VALUE FOR PIPE CONNECTION SCENARIO WITHOUT CONTROLLER

Number of Cells	K_G (after $t \geq 0.5h$)		K_L (after $t \geq 0.5h$)	
	UKF	EKF	UKF	EKF
6	1.4×10^{-3}	1.6×10^{-3}	3.7×10^{-3}	3.8×10^{-3}
12	1.9×10^{-3}	2.2×10^{-3}	3.9×10^{-3}	3.9×10^{-3}
20	2.4×10^{-3}	3.1×10^{-3}	4.8×10^{-3}	5.0×10^{-3}

effect on the estimation of production indices. Therefore these methods with different number of spatial discretization cells are very sensitive to errors in the reservoir pore pressure value. The results show that UKF and EKF with different number of spatial discretization cells are robust in case of error in the liquid density value of the model.

V. Conclusion

In this paper, the joint UKF and EKF have been applied to the drift-flux model for different spatial discretization cells to estimate the distributed unmeasured states, geological properties of the reservoir (production index) and slip parameters (S, K) during UBD operations using measurement of the bottom-hole pressure and liquid and gas rate at the outlet. Furthermore, both production indices of gas and liquid and unmeasured states were estimated by using only measurements of the choke and the bottom-hole pressures for the pipe connection procedure. Simulation results demonstrated reasonable performance of the joint UKF and EKF to detect and track a changing gas production coefficient using the simulated scenario with OLGA. Even though the simulation scenario is somewhat idealized the results are encouraging. The number of spatial discretization cells was found to not have a significant effect on accuracy of estimation. The UKF was also found to estimate more accurately than the EKF. The results show that these methods are very sensitive to errors in the reservoir pore pressure value. However, the methods are robust in case of error in the liquid density value of the model.

Since some type of MWD (i.e. Wired Drill Pipe or Mud Pulse Telemetry) loses down hole data for a few minutes for each connection, the future research could be to evaluate these proposed methods with missing down hole data.

Acknowledgment

The authors gratefully acknowledge the financial support provided to this project through the Norwegian Research Council and Statoil ASA (NFR project 210432/E30 Intelligent Drilling).

The second author was also supported by the Research Council of Norway, ConocoPhillips, Det norske oljeselskap, Lundin, Statoil and Wintershall through the research center DrillWell (Drilling and Well Centre for Improved Recovery) at IRIS.

We would like to thank Florent Di Meglio for his contribution to the modeling. We would like to thank Esmaeil Jahanshahi for his contribution for OLGA simulation.

References

[1] J.-M. Godhavn, "Control requirements for automatic managed pressure drilling system," *SPE Drilling & Completion*, vol. 25, no. 3, pp. 336–345, September 2010.

[2] A. Nikoofard, T. A. Johansen, H. Mahdianfar, and A. Pavlov, "Constrained mpc design for heave disturbance attenuation in offshore drilling systems," in *OCEANS-Bergen, 2013 MTS/IEEE*, 2013, pp. 1–7.

[3] D. Bennion, F. Thomas, R. Bietz, and D. Bennion, "Underbalanced drilling, praises and perils," in *Permian Basin Oil and Gas Recovery Conference*, 1996.

[4] U. J. F. Aarsnes, F. D. Meglio, R. Graham, and O. M. Aamo, "A methodology for classifying operating regimes in underbalanced drilling operations," *SPE J.*, 2016.

[5] S. Evje and K. K. Fjelde, "Hybrid flux-splitting schemes for a two-phase flow model," *Journal of Computational Physics*, vol. 175, pp. 674–701, 2002.

[6] R. Lorentzen, G. Nævdal, and A. Lage, "Tuning of parameters in a two-phase flow model using an ensemble kalman filter," *International Journal of Multiphase Flow*, vol. 29, no. 8, pp. 1283–1309, August 2003.

[7] A. Lage, E. Nakagawa, R. Time, E. Vefring, and R. Rommetveit, "Full-scale experimental study for improved understanding of transient phenomena in underbalanced drilling operations," in *SPE/IADC Drilling Conference*, no. 52829-MS. Amsterdam, Netherlands: Society of Petroleum Engineers, March 1999.

[8] G. Nygaard and G. Nævdal, "Nonlinear model predictive control scheme for stabilizing annulus pressure during oil well drilling," *Journal of Process Control*, vol. 16, no. 7, pp. 719–732, August 2006.

[9] A. Nikoofard, T. A. Johansen, and G.-O. Kaasa, "Design and comparison of adaptive estimators for under-balanced drilling," in *American Control Conference (ACC)*, Portland, Oregon, USA, June 2014, pp. 5681–5687.

[10] E. Storkaas, S. Skogestad, and J.-M. Godhavn, "A low-dimensional dynamic model of severe slugging for control design and analysis," in *11th International Conference on Multiphase flow (Multiphase03)*, 2003, pp. 117–133.

[11] G. Nygaard, G. Nævdal, and S. Mylvaganam, "Evaluating nonlinear kalman filters for parameter estimation in reservoirs during petroleum well drilling," in *Computer Aided Control System Design, 2006 IEEE International Conference on Control Applications, 2006 IEEE International Symposium on Intelligent Control*. IEEE, 2006, pp. 1777–1782.

[12] G. H. Nygaard, L. S. Imsland, and E. A. Johannessen, "Using nmpc based on a low-order model for controlling pressure during oil well drilling," in *8th International IFAC Symposium on Dynamics and Control of Process Systems*, vol. 1, Mexico, June 2007, pp. 159–164.

[13] A. Nikoofard, T. A. Johansen, and G.-O. Kaasa, "Evaluation of lyapunov-based adaptive observer using low-order lumped model for estimation of production index in under-balanced drilling," in *9th International Symposium on Advanced Control of Chemical Processes (ADCHEM)*. Whistler, British Columbia, Canada: IFAC, June 2015, pp. 69–75.

[14] ——, "Nonlinear moving horizon observer for estimation of states and parameters in under-balanced drilling operations," in *ASME 2014 Dynamic Systems and Control Conference*. American Society of Mechanical Engineers, 2014.

[15] E. H. Vefring, G. Nygaard, R. J. Lorentzen, G. Nævdal, K. K. Fjelde *et al.*, "Reservoir characterization during ubd: Methodology and active tests," in *IADC/SPE Underbalanced Technology Conference and Exhibition*. Society of Petroleum Engineers, 2003.

[16] E. H. Vefring, G. H. Nygaard, R. J. Lorentzen, G. Naevdal, K. K. Fjelde *et al.*, "Reservoir characterization during underbalanced drilling (ubd): methodology and active tests," *SPE Journal*, vol. 11, no. 02, pp. 181–192, 2006.

[17] U. J. F. Aarsnes, O. M. Aamo, F. Di Meglio, and G.-O. Kaasa, "Fit-for-purpose modeling for automation of underbalanced drilling operations," in *SPE/IADC Managed Pressure Drilling & Underbalanced Operations Conference & Exhibition*. Society of Petroleum Engineers, 2014.

[18] R. A. Graham and M. S. Culen, "Methodology For Manipulation Of Wellhead Pressure Control For The Purpose Of Recovering Gas To Process In Underbalanced Drilling Applications," in *Proc. SPE/IADC Underbalanced Technol. Conf. Exhib.* Houston, Texas: Society of Petroleum Engineers, Oct. 2004.

[19] U. J. F. Aarsnes, F. Di Meglio, S. Evje, and O. M. Aamo, "Control-oriented drift-flux modeling of single and two-phase flow for drilling," in *ASME 2014 Dynamic Systems and Control Conference*. American Society of Mechanical Engineers, October 2014.

[20] F. Di Meglio, D. Bresch-Pietri, and U. J. F. Aarsnes, "An adaptive observer for hyperbolic systems with application to underbalanced drilling," in *IFAC World Congress 2014*, 2014, pp. 11 391–11 397.

[21] G. Li, H. Li, Y. Meng, N. Wei, C. Xu, L. Zhu, and H. Tang, "Reservoir characterization during underbalanced drilling of horizontal wells based on real-time data monitoring," *Journal of Applied Mathematics*, vol. 2014, 2014.

[22] D. Simon, *Optimal state estimation: Kalman, H infinity, and nonlinear approaches*. Wiley. com, 2006.

[23] E. A. Wan and R. van der Merwe, *The Unscented Kalman Filter, in Kalman Filtering and Neural Networks (ed S. Haykin)*. New York, USA: John Wiley & Sons, March 2002, ch. 7.

[24] A. Nikoofard, U. J. F. Aarsnes, T. A. Johansen, and G.-O. Kaasa, "Estimation of states and parameters of drift-flux model with unscented kalman filter," in *Proceedings of the 2015 IFAC Workshop on Automatic Control in Offshore Oil and Gas Production*, vol. 2, Florianópolis, Brazil, May 2015, pp. 171–176.

[25] S. Evje, "Weak solutions for a gas-liquid model relevant for describing gas-kick in oil wells," *SIAM Journal on Mathematical Analysis*, vol. 43, no. 4, pp. 1887–1922, 2011.

[26] H. Shi, J. A. Holmes, L. J. Durlofsky, K. Aziz, L. Diaz, B. Alkaya, G. Oddie *et al.*, "Drift-flux modeling of two-phase flow in wellbores," *Spe Journal*, vol. 10, no. 01, pp. 24–33, 2005.

[27] S. J. Julier, J. K. Uhlmann, and H. F. Durrant-Whyte, "A new method for the nonlinear transformation of means and covariances in filters and estimators," *IEEE Transactions on Automatic Control*, vol. 45, no. 3, pp. 477–482, March 2000.

[28] S. J. Julier and J. K. Uhlmann, "Unscented filtering and nonlinear estimation," *Proceedings of the IEEE*, vol. 92, no. 3, pp. 401 – 422, March 2004.

[29] R. van der Merwe, "Sigma-point kalman filters for probabilistic inference in dynamic state-space models," Ph.D. dissertation, Oregon Health & Science University, April 2004.

[30] S. Shayegi, C. S. Kabir, S. Christensen, K. Kosco, J. Casasus-Bribian, K. Hasan, and H. Moos, "Reservoir characterization begins at first contact with the drill bit," in *IPTC 2012: International Petroleum Technology Conference*, 2012.

[31] M. S. Culen, D. R. Killip *et al.*, "Forensic reservoir characterisation enabled with underbalanced drilling," in *SPE European Formation Damage Conference*. Society of Petroleum Engineers, 2005.

[32] K. H. Bendiksen, D. Maines, R. Moe, S. Nuland *et al.*, "The dynamic two-fluid model olga: Theory and application," *SPE production engineering*, vol. 6, no. 02, pp. 171–180, 1991.

[33] U. J. F. Aarsnes, "Modeling of Two-Phase Flow for Estimation and Control of Drilling Operations," Ph.D. dissertation, Norwegian University of Science and Technology, 2016.

[34] A. Nikoofard, T. A. Johansen, H. Mahdianfar, and A. Pavlov, "Design and comparison of constrained mpc with pid controller for heave disturbance attenuation in offshore managed pressure drilling systems," *Marine Technology Society Journal*, vol. 48, no. 2, pp. 90–103, 2014.

[35] G. Nygaard and G. Nævdal, "Modelling two-phase flow for control design in oil well drilling," in *Control Applications, 2005. CCA 2005. Proceedings of 2005 IEEE Conference on*. IEEE, 2005, pp. 675–680.